

Magnetic resonance in the spin-glass $(LaGd)Al_2$

M. Zomack and K. Baberschke

*Institut für Atom- und Festkörperphysik, Freie Universität Berlin,
Arnimallee 14, D-1000 Berlin 33, Federal Republic of Germany*

S. E. Barnes

*Physics Department, University of Miami, P.O. Box 248046,
Coral Gables, Florida 33124*

(Received 14 June 1982; revised manuscript received 29 November 1982)

ESR has been measured in the spin-glass $(La_{1-x}Gd_x)Al_2$, $1 \leq x \leq 15$ at. % for 1, 3, 9, and 35 GHz, corresponding to different applied magnetic fields and in the temperature range of 100 mK to 30 K. The comparison of data for different frequencies shows that the linewidth depends very much on the frequency and/or field and therefore the temperature T_{\min} of the linewidth minimum is not an intrinsic parameter and the shift of the resonance position is almost independent of frequency. The former effect is analyzed and theoretically explained in terms of the temperature dependence of the measured susceptibility at the field for resonance instead of a Curie-Weiss susceptibility. When the resonance position does shift, close to the glass temperature, this is identified to be an internal-field, rather than a g -factor, effect. The temperature dependence of this internal field differs from that of the bulk magnetization.

I. INTRODUCTION

Recently, electron spin resonance (ESR) in spin-glasses has attracted increased interest. Experiments and theory can be crudely divided into two groups: First, experiments for which the temperature $T \ll T_C$, the glass temperature. Here interest is in the position of the resonance signal which is discussed as a function of field history and for different frequencies, etc. The prototype for these experiments is the $CuMn$ work by Monod *et al.*¹ and the detection of a second resonance mode ω^- by Schultz *et al.*² and last but not least the pioneer work of all ESR in metals by Owens *et al.*³ In this regime ESR probes the resonant magnetization and its anisotropy as suggested by Fert *et al.*⁴; the latter probably arises from a second-order effect of exchange and spin-orbit interactions producing a Dzyaloshinsky-Moriya interaction (DM).

The second group of experiments (our present work) is related to the temperature range where $T > T_C$ or $T \sim T_C$. Coming from the paramagnetic regime ($T \gg T_C$) the change of the linewidth and shift of the resonance signal seems to carry important information. Motivation for such work includes the proposal of Salamon *et al.*⁵ that the relaxation rate should exhibit critical power-law behavior near T_C . Among the many and varied

studies are $CuMn$,^{5,6} $AgMn$,^{7,8} $AuMn$,⁹ and $AuFe$,¹⁰ along with a host of rare-earth spin-glasses; to name only a few: amorphous $AlGd$,¹¹ $(LaGd)Al_2$,¹² and $(YGd)Al_2$.¹³

What has been accomplished to date demonstrates that ESR can provide valuable information about spin-glass properties. However, many uncertainties remain in the interpretation of the experiments performed on our regime of interest, $T \gtrsim T_C$. The origin of the dramatical change in the field for resonance and linewidth while decreasing the temperature is unclear. Is there a "field shift" or a "g shift"¹² and what is the meaning of the additional linewidth? It might be that for interacting systems a distribution of internal anisotropic magnetizations simply smears out of the resonance condition¹³ and therefore the observed linewidth may have nothing to do with dynamic properties and in particular with critical phenomena.^{5,6} Furthermore, in our temperature regime $10^{-1} < T/T_C < 2$ it remains an open question whether we observe a single-ion "paramagnetic" resonance or some kind of $q=0$ spin wave arising from strongly coupled moments.

The present investigation tries to shed some light in this area by performing the same ESR experiment on the same sample at different frequencies. We have available 1, 3, 9, and 35 GHz to which the corresponding field for $g=2$ is approximately 350 G,

1000 G, 3300 G, and 12.5 kG.

In ESR one has to change simultaneously the applied field, which influences many spin-glasses, but also the frequency, that is, the time window. This is important since the definition of static and dynamic depends on whether the spin-fluctuation rates τ_s^{-1} are fast or slow compared to the Lamor frequency ω_L and also since for our system it has been claimed that there should be a relatively strong frequency dependence of the glass phenomena.¹⁴

Specifically the system $(LaGd)Al_2$ was chosen because it has been extensively studied and since it is suitable for the present ESR work. Löhneysen *et al.* measured the magnetic properties,¹⁵ their frequency,¹⁴ and time dependence.¹⁶ In addition, ESR of the dilute limit is well known, the exchange coupling^{17,18} has been measured, and it is known that the single-ion crystal-field splitting¹⁹ is small.

In the following we first describe (after experimental details) the high-temperature behavior ($T \gg T_C$) of the linewidth (Sec. III) and field for resonance (Sec. IV) with explanations for an observed negative residual linewidth¹⁰ and a negative g shift.²¹ Section V presents the results for $T \gtrsim T_C$. The principal thrust of this work is to show undoubtedly for the first time that the shift of the resonance signal is essentially a field effect and not a g shift; it is almost independent of ν_0 and only a function of T . In contrast, the linewidth depends very much on ν_0 ; we find that T_{\min} , the temperature for minimum linewidth, has no intrinsic meaning. We are able to theoretically analyze the line broadening for $T \gtrsim T_C$ by introducing the experimental susceptibility into the Bloch-Hasegawa equations. The spin-glass phenomena in the ESR linewidth is shown to enter via the susceptibility.²² In Sec. VI we will present some low-temperature results for the 6-at. % sample for $100 \text{ mK} \leq T \leq 4 \text{ K}$. The ESR does not show a second mode or any field cooling or time effects. Section VII contains a discussion of our results.

II. EXPERIMENTAL DETAILS

The resonance spectrometer is of conventional type in the reflection mode using the most common microwave frequencies of 9 and 36 GHz (Varian), 1 and 3 GHz (Bruker). Note the enormous influence of the applied field on the χ_{ac} measurements (Fig. 4 in Ref. 15). For different ranges in temperature we used He-gas-flow systems, a liquid-He cryostat, and for very low temperatures ($T < 1 \text{ K}$), a ^3He - ^4He dilution refrigerator²³ (see Sec. VI).

The samples were prepared by induction and arc melting. All the performed checks concerning the structural homogeneity of the samples, i.e., the x-ray width of superconducting transition temperature

(for very low concentrations) show a homogeneous structure of the cubic $C15$ Laves phase and a random distribution of Gd on the La sites. Also from physical reasons, i.e., the resemblance of atomic radii, valence, and chemical potential, this substitution should proceed without any problem. This is not guaranteed in all cases for spin-glasses where $3d$ ions are diluted in a Cu, Ag, or Au matrix. Recent extended x-ray-absorption fine-structure (EXAFS) studies for $(LaGd)Os_2$ (Ref. 24) and small-angle x-ray scattering in $AuFe$ (Ref. 25) confirm these statements. We will come back to this point in Sec. VII. Different sample shapes were used (cylinders for the refrigerator experiments and some buttons), but mostly we measured the samples in powder form.

This brings up the question of *demagnetization effects*, a very basic effect and carefully discussed in early papers on ESR.²⁶ Since this effect can produce shifts and line broadening, we present the details in Appendix A. In short, (i) for powder grains as for spheres we assume that $H_{\text{loc}} = H_{\text{ext}}$, the external field. (ii) We do see resonance shifts for cylindrical samples with respect to the value obtained in the powder experiment. This shift agrees with the calculated demagnetization field for the given geometry. The experimental data in Sec. VI are corrected for this field. (iii) Nevertheless, in powder we do have different shapes and demagnetization factors for different grains. The random distribution of different grains deforms the line shape and broadens (inhomogeneously) the linewidth.²⁷

In Fig. 1 we show *magnetization* measurements

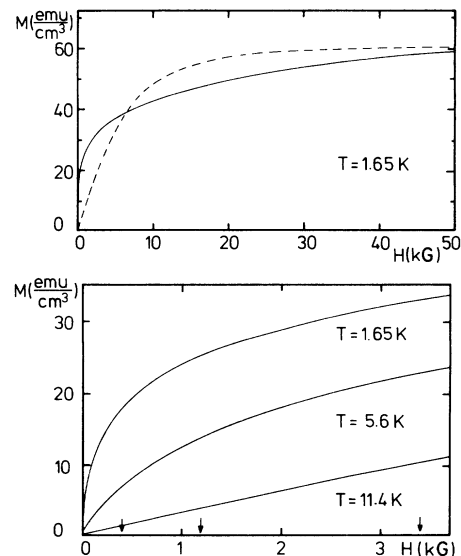


FIG. 1. Magnetization of $(La_{0.94}Gd_{0.06})Al_2$. (a) Shows the behavior in high fields; the dashed line is a Brillouin function with $g = 2.1$. (b) Shows the behavior in the field regime which is used in resonance experiments.

for the 6-at. % sample. Figure 1(a) demonstrates the deviations from a Brillouin-type (dashed line) behavior and the Matho-Larkin^{28,29} contribution in agreement with previous experiments.¹⁵ Figure 1(b) shows the magnetization for different temperatures and in the relevant field range for the L , S , and X , bands. This becomes important in Sec. V where we demonstrate that in the Bloch-Hasegawa equations the static susceptibility of the system enters. Since there exists no complete calculation of $M(H, T)$ for arbitrary H , and T in a spin-glass, we use

$$\chi^{\text{expt}} = M(H_{\text{ext}}, T) / H_{\text{ext}}$$

and the differential susceptibility

$$\tilde{\chi}(H_{\text{ext}}) = \frac{\partial M(H_{\text{ext}}, T)}{\partial H}$$

from the experiment for each sample. This is one important mechanism by which the spin-glass property enters into the dynamics of the ESR (Secs. V and VII).

Typical ESR spectra with almost perfect Dysonian line shape³⁰ and a large deviation from it are shown in Fig. 2. The principal parameters with which we want to describe the spectra are the linewidth full width at half maximum (FWHM) ΔH and the resonance shift δH_{res} . To show the results for different frequencies in one diagram we plotted

$$\delta H_{\text{res}} = H_{\text{expt}} - H(g = 1.993), \quad (1)$$

the shift with respect to the Gd resonance in insulators.

As one can see from Fig. 2 the experimental line shape in some cases does not coincide with a Dysonian. This enlarges the error bar for H_{res} and ΔH . We justify our analysis in the following way: (i) We found that line shapes for the 1- and 3-GHz experiments are more Dysonian than at 9 and 35 GHz; for the latter we found systematic deviations, namely less intensity in the high- and low-field wings. Because of this error source we give for the X band as a maximal absolute error $\pm 10\%$ for ΔH and $\pm 15\%$ for δH_{res} . The relative error is smaller by approximately a factor of 3. It is worthwhile to mention in connection with the skin-depth problem that we did not vary the admixture of χ' and χ'' . All data were fitted with a fixed ratio $A/B = 2.53$. For our samples we are in the limit of mean free path of the conduction electrons (CE) \ll skin depth \ll sample size. This condition forces a pure paramagnetic resonance to a perfect Dysonian line shape with a fixed ratio $A/B = 2.53$.³⁰ This has been recently experimentally proven by low-frequency ESR.³¹ One is therefore forced to explain line-shape effects in other terms than skin-depth effects.

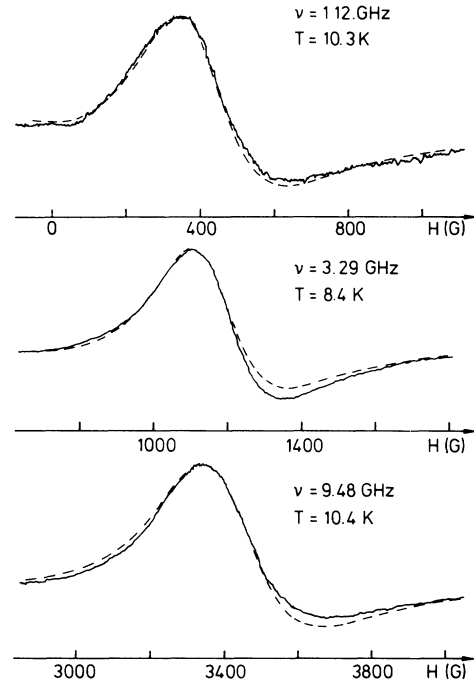


FIG. 2. Experimental resonance curves of $(La_{1-x}Gd_x)Al_2$, $x = 0.03$. Dashed lines are calculated Dysonian line shapes.

Fortunately, the two main results of the present investigation, that is, the field shift in the resonance field and the field- (frequency-) dependent broadening of the linewidth, are 1 order of magnitude larger than changes due to the modified shape.

III. EXPERIMENTAL RESULTS AND THEORETICAL ANALYSIS FOR $T \gg T_c$

In Fig. 3 we show an overview of the ESR linewidth versus the temperature in the concentration range of 1–15 at. %. In this section we will analyze the results for high temperature, that is, the regime of linear thermal broadening. Figure 3 shows clearly that for 1 at. % (up to 5 at. %, see Table I) the system is in the intermediate bottleneck regime: With increasing concentration of Gd, the thermal broadening b decreases. In contrast to $CuMn$, where the linewidth versus temperature approaches almost a horizontal line, $b < 2$ G/K, for $(LaGd)Al_2$, $b \cong 8$ G/K becomes constant for $c \geq 6$ at. %. This is associated with the finite spin-orbit scattering of the CE at the Gd^{3+} impurities. Since the spin-orbit interaction is a possible source for anisotropy energy (DM and pseudodipolar⁴) in spin-glasses, and since ESR provides an excellent tool to measure the spin-orbit scattering we will briefly re-

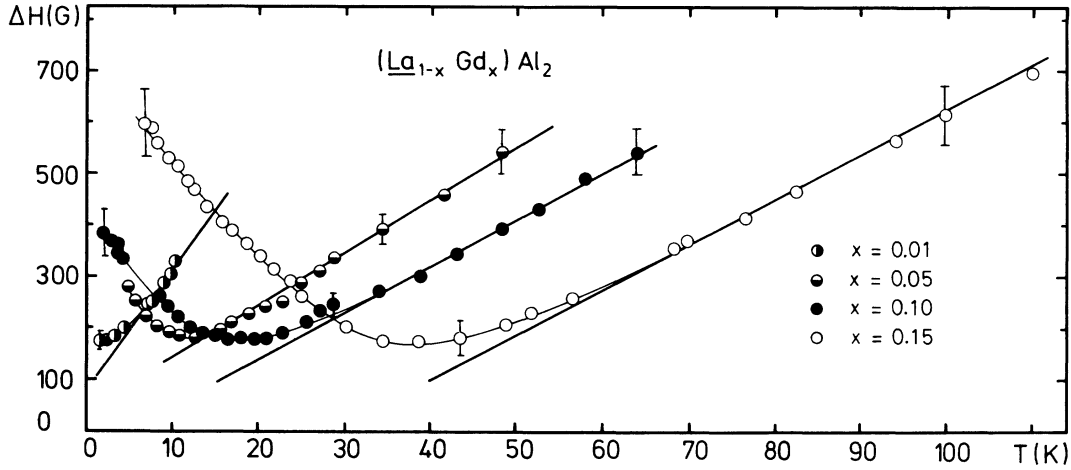


FIG. 3. Linewidth vs temperature for $(\text{Gd}_x\text{La}_{1-x})\text{Al}_2$, with $x=1$ at. % (\bullet), 5 at. % (\circ), 10 at. % (\bullet), and 15 at. % (\circ) at 9 GHz. Solid lines at low T are guide for the eyes.

call how it enters in the theoretical description of ESR: In metals the observed signal corresponds to the common resonance of two distinct subsystems—the CE and the local moments. In the isothermal case the relaxation of the CE spins is dominated by the spin-orbit coupling to the lattice. In the opposite limit where exchange scattering overcomes the spin-orbit scattering the CE and local moments form a dynamically strong coupled resonance system, the so-called bottleneck. As for strongly coupled pendulums, the eigenfrequencies are affected. The degree of bottleneck³² is characterized by $\delta_{eL}/(\delta_{ei} + \delta_{eL})$ which is 1 for the isothermal limit and 0 in the extreme bottleneck.³³ We have

$$\delta_{eL} = \delta_{eL}^0 + \delta'_{eL} x_{\text{imp}}, \quad (2)$$

the sum of an inherent contribution from the host (imperfections of the host) and a term proportional

to the Gd concentration (Gd acts as an imperfection on a La site). In contrast, δ_{ei} (the so-called Overhauser rate) depends only on x_{Gd} . In view of our spin-glass properties the former rate, δ_{eL} , is more important. It is exact the parameter which enters into the calculation by Fert and Levy.⁴ We will return to this point (Sec. VII) and focus in this section on the analysis of the data.

The bottleneck parameter $\delta_{eL}/(\delta_{ei} + \delta_{eL})$ becomes independent of the Gd concentration x when $\delta_{eL}^0 < \delta'_{eL} x$ where $\delta_{eL}^0 \cong 6 \times 10^{11} \text{ sec}^{-1}$ is the intrinsic spin-orbit scattering of the pure host matrix, LaAl_2 , and δ'_{eL} is the additional rate per Gd concentration. This yields $\delta'_{eL} \geq 1 \times 10^{11} \text{ sec}^{-1}/1 \text{ at. \% Gd}$. These results agree with previous experiments.^{32,34} As can be seen from the last two columns of Table I, including the δ'_{eL} considerably alters the predicted thermal broadening; the agreement with the experimental data of column 3 is good. In Figs. 4–7 we

TABLE I. Various experimental values and theoretical results. Columns 2 and 3 show the experimental values for the thermal broadening b (for high T up to 60 K) and the residual linewidth a according to Eq. (3). T_{min} is defined by the temperature where the minimum in the observed linewidth occurs. Θ_P is the paramagnetic Curie temperature, taken from Ref. 36. Column 8 shows the calculated values for a according to Eq. (12). b (columns 9 and 10) is determined by the usual bottleneck formula $b = \delta_{ei}/(\delta_{ei} + \delta_{eL})b_K$. For a_0 , b_K , and δ_{ei}^0 we took the values of the dilute limit (17a): $a_0 = 150 \text{ G}$, $b_K = 60 \text{ G/K}$, and $\delta_{ei}^0 = 6 \times 10^{11} \text{ sec}^{-1}$.

x (at.%)	a (G)	b (G/K)	T_{min} (K)			Θ_P (K) (Ref. 36)	$a = a_0 - b\Theta_P$	$b = \delta_{ei}/(\delta_{ei} + \delta_{eL})b_K$ with	
			1 GHz	3 GHz	9 GHz			$\delta_{ei} = \delta_{ei}^0 = \text{const}$	$\delta_{ei} = \delta_{ei}^0 + \delta'_{ei}$
1	80 ± 20	24 ± 2			< 2	4 ± 3	35 ± 70	24	26.2
3	77 ± 20	19 ± 2	3.7	4.4	5.2 ± 1	5 ± 2	34 ± 40	10.9	16.3
5	35 ± 20	10.5 ± 1			13 ± 1.5	7.5 ± 2	71 ± 20	7.1	11.8
6	45 ± 20	8.9 ± 1	6.9	9.0	12.5 ± 1.5	9 ± 2	70 ± 20	6.0	10.9
8	0 ± 20	7.7 ± 1	10	13	16.5 ± 2	12 ± 2	57 ± 20	4.6	10.5
10	-40 ± 20	9.0 ± 1			19.5 ± 2	14 ± 2	24 ± 20	3.8	9.1
15	-240 ± 20	8.6 ± 1		33	39 ± 3	26 ± 3	-74 ± 30	2.8	8.0

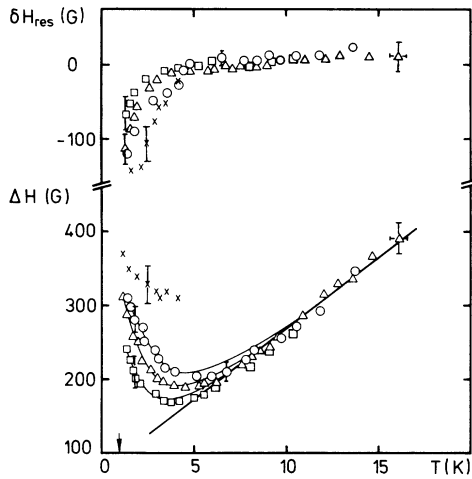


FIG. 4. Linewidth ΔH and the deviation of resonance field (see Sec. II) for $(Gd_{0.03}La_{0.97})Al_2$. Frequencies are 1 GHz (\square), 3.3 GHz (Δ), 9.3 GHz (\circ), and 34 GHz (\times). Arrow shows T_C (16 Hz) (see Sec. VII). Solid lines at low T are guide for the eyes.

show the detailed results for ΔH and δH_{res} for various concentrations. In the high-temperature regime the field for resonance H_{res} is almost independent of temperature and corresponds to a g value of approx-

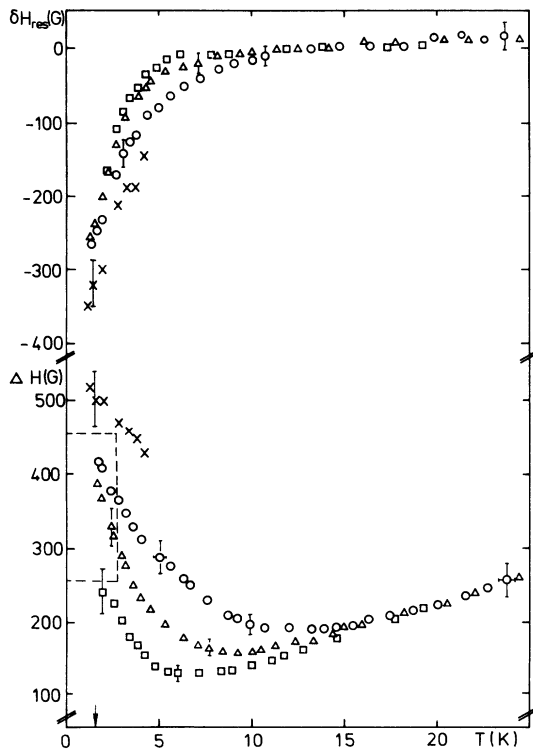


FIG. 5. Linewidth and deviation of resonance field for $(Gd_{0.06}La_{0.94})Al_2$. For symbols see Fig. 4. For detailed results below 2.5 K see Fig. 11.

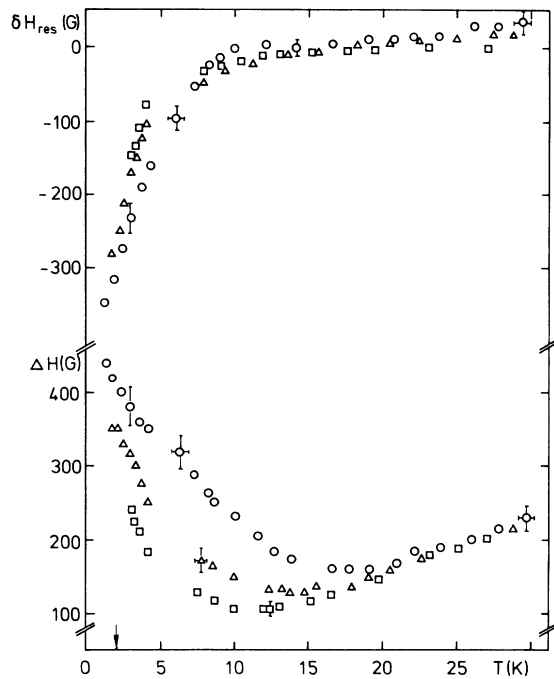


FIG. 6. Linewidth and deviation of resonance field for $(Gd_{0.08}La_{0.92})Al_2$. For symbols see Fig. 4.

imately 1.993. For comparison with experiments for different microwave frequencies we plot $\delta H_{res} = H_{res}^{expt} - H_{res}^{g=1.993}$. At high temperatures where δH_{res} approaches a temperature-independent limit small but systematic differences can be seen.

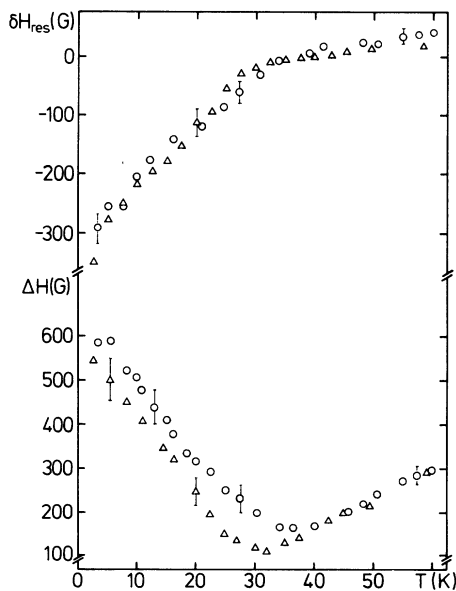


FIG. 7. ΔH and δH_{res} for $(Gd_{0.15}La_{0.85})Al_2$; for symbols see Fig. 4. For this sample the line shape deviates strongly from Fig. 2. Possibly this is due to the onset of long-range interactions.

The data for higher frequencies (\circ, \triangle) lie always above that for the low frequency (\square). This is indicative of a g shift with g values smaller than $g^{\text{ionic}} = 1.993$. We will discuss this in Sec. IV.

We now turn to the linewidth for the high-temperature limit. In this section we will analyze the linewidth in the commonly accepted way, namely in terms of the formula

$$\Delta H = a + bT. \quad (3)$$

No frequency or field dependence is observed and the thermal broadening is linear in T . In Table I we summarize the a and b parameters. The residual linewidth a contains two contributions: (i) For low concentrations it is constant,¹⁷ $a = a_0 \cong 150$ G. This is attributed to a residual linewidth (not relaxation) due to crystal-field effects and local imperfection through the DM mechanism. It will be included in the Bloch-Hasegawa equation as a local moment to lattice-relaxation rate δ_{iL} [read in the other notation as $1/T_{sL}$ (Ref. 33)]. That this is justified for what is essentially an inhomogeneous field distribution is shown in Appendix B. (ii) A concentration-dependent term which becomes important for larger Curie-Weiss constants. This will be explained in the following.

ESR in alloys such as ours for high temperatures $T \gg T_C$ is usually understood in terms of the Bloch-Hasegawa equations. However, despite the frequent application of this theory to a variety of systems there still exist some subtleties which have not really surfaced in the experimental literature. One such subtlety is the dependence of the residual width upon the Curie-Weiss constant Θ .

The Bloch-Hasegawa equations are

$$\begin{aligned} \frac{d\vec{M}_i}{dt} = & g_i \mu_B [\vec{M}_i \times (\vec{H}_{\text{ext}} + \lambda \vec{M}_e + \alpha \vec{M}_i)] \\ & - (\delta_{ie} + \delta_{iL}) \delta \vec{M}_i + \frac{g_i}{g_e} \delta_{ei} \delta \vec{M}_e, \end{aligned} \quad (4)$$

$$\begin{aligned} \frac{d\vec{M}_e}{dt} = & g_e \mu_B [\vec{M}_e \times (\vec{H}_{\text{ext}} + \lambda \vec{M}_i)] \\ & - (\delta_{ei} + \delta_{eL}) \delta \vec{M}_e + \frac{g_e}{g_i} \delta_{ie} \delta \vec{M}_i, \end{aligned} \quad (5)$$

$$\delta_{eL} [M_e^+ - \chi_e^0 (h_{\text{rf}} + \lambda M_i^+)] \cong \delta_{eL} \left[\frac{\chi_e}{\chi_i + \chi_e} M^+ - \lambda \chi_e^0 \frac{\chi_i}{\chi_i + \chi_e} M^+ - \chi_e^0 h_{\text{rf}} \right] \pm \delta_{eL} \frac{\chi_e^0}{\chi_i + \chi_e} [M^+ - (\chi_i + \chi_e) h_{\text{rf}}], \quad (10)$$

where the fact that in the numerator χ_e is replaced by χ_e^0 in the last line is of central importance. This follows from Eq. (9). Thus the electron lattice-relaxation rate δ_{eL} contributes an amount

where

$$\delta \vec{M}_i = [\vec{M}_i - \chi_i^0 (\vec{H}_{\text{ext}} + \lambda \vec{M}_e + \alpha \vec{M}_i)] \quad (6)$$

and

$$\delta \vec{M}_e = [\vec{M}_e - \chi_e^0 (\vec{H}_{\text{ext}} + \lambda \vec{M}_i)]. \quad (7)$$

For high temperatures the susceptibility is of Curie-Weiss form and is given by the following molecular-field equations:

$$\chi_i = \chi_i^0 (1 + \lambda \chi_e + \alpha \chi_i) \quad (8)$$

and

$$\chi_e = \chi_e^0 (1 + \lambda \chi_i), \quad (9)$$

and where

$$\chi_i^0 = \frac{c}{3} (g_i \mu_B)^2 [(S+1)/kT]$$

and

$$\chi_e^0 = \frac{1}{2} (g_e \mu_B) \rho (E_F)$$

are the susceptibilities per site for a concentration c . Introduction of the constant α gives independent Curie $C = (1 + 2\lambda \chi_e^0) (\chi_i^0 T)$ and Curie-Weiss $\Theta = (\lambda^2 \chi_e^0 + \alpha) (\chi_i^0 T)$ constants.³⁵

When linearized, Eqs. (4) and (5) reduce to a quadratic equation. However, in certain limits one can follow a more direct and physical approach. For zero lattice relaxation $\delta_{eL} = \delta_{iL} = 0$, the bottleneck limit, one has that the total transverse magnetization $M^+ = M_e^+ + M_i^+$ precesses with the rf field. It follows that

$$M_i^+ = [\chi_i / (\chi_i + \chi_e)] M^+$$

and

$$M_e^+ = [\chi_e / (\chi_i + \chi_e)] M^+$$

are the zeroth-order eigenvector. The first-order correction is obtained by substituting this eigenvector in the equation for M^+ [obtained by adding Eqs. (4) and (5)] but with δ_{eL} and δ_{iL} not zero. Of particular interest is the term

$$\delta_{eL} \frac{\chi_e^0}{\chi_i + \chi_e} \cong \delta_{eL} \frac{\chi_e^0}{\chi_i} = \delta_{eL} \frac{\chi_e^0}{C} (T - \Theta)$$

to the relaxation rate of the total magnetization.

Passing to the right, first the approximation $\chi_e \ll \chi_i$ has been used, then the Curie-Weiss form $\chi_i = C/(T - \Theta)$ has been substituted. The total effective relaxation rate for the bottleneck mode is

$$\delta = \left[\frac{\chi_i^0 \delta_{iL} + \chi_e^0 \delta_{eL}}{\chi_i + \chi_e} \right] \cong \delta_{iL} \chi_i^0 \chi_i^{-1} + \delta_{eL} \chi_e^0 C^{-1} (T - \Theta), \quad (11a)$$

$$\hbar \delta / g \mu_B \cong \Delta H \cong a + bT, \quad (11b)$$

where

$$a = \hbar \delta_{iL} g \mu_B \cong a_0 - b\Theta \quad (12)$$

and

$$b = \delta_{eL} \chi_e^0 C^{-1} \hbar / g \mu_B \cong \delta_{eL} / \delta_{ei} b_K. \quad (13)$$

Generally, b is the experimentally determined broadening (G/K) and b_K the unbottlenecked Korringa rate.

In the preceding paragraph we have assumed a full bottleneck. Nevertheless, Eq. (12) also holds for the isothermal limit. The formula for the constant a demonstrates its dependence upon Θ . Clearly there is the possibility that a may be negative as is found for some of our samples. We find qualitative agreement between columns 2 and 8 in Table I. A more quantitative agreement depends on the knowledge of Θ . We used the paramagnetic Θ_p (Ref. 36).

IV. NEGATIVE g SHIFT AND POSITIVE J_{kf}

Before we turn to the analysis of the low-temperature data we want to complete the analysis for $T \gg T_C$. H_{res} for the 8-at. % sample and temperatures $T > 25$ K yields a g value of $g_{exp} \cong 1.97$. This is a clear g -shift effect as can be seen in Fig. 6; for large resonance frequencies (\circ, \triangle) the line shifts more than for the low frequency (\square). This is in qualitative agreement with numerous publications on the ESR of GdAl₂.^{26,37} The conventional way of analyzing this figure is to compare it with $g_{ionic} = 1.993$ and to attribute the negative shift to a negative exchange interaction or within a two-band model to one contribution of it.³⁸ Very recently Zipper proposed an alternative explanation²⁷ which works for bottleneck systems like GdAl₂. Many of the highly concentrated alloys (see Table 3 in Ref. 38) are bottlenecked. She pointed out that the former interpretation is faced with the contradiction of negative J_{kf} but larger saturation magnetization than for free ions $M_s > 7\mu_B/\text{Gd atom}$ (see Fig. 1 and Ref. 15). We will briefly recall her²⁷ arguments because of their importance in understanding the ESR completely and they bring into play again the spin-orbit coupling.⁴

Band-structure calculations³⁹ show that the electron states at E_F do have large d -band character from the La site. It is natural, therefore, to treat the Zeeman effect for the conduction band as

$$(g \vec{1} + g_{fr} \vec{\sigma}) \cdot \vec{H} + \sum \xi \vec{1} \cdot \vec{\sigma}, \quad (14)$$

including the spin-orbit interaction. One might think of a tight-binding La d band constructed out of orbitals very similar to those for $3d$ ions in insulators. Under certain assumptions and for the lowest-lying cubic crystalline electric field Γ_3 , second-order perturbation theory yields an effective g factor for d -band electrons. We have

$$g_d = g_{fr} (1 - \xi_0 \Lambda^z) \simeq g_{fr} (1 - \bar{\xi} / \Delta \epsilon), \quad (15)$$

where $g_{fr} = 2$ is the g value of the free-electron gas, ($\bar{\xi}$), ξ_0 is the (mean) spin-orbit coupling, and $\Delta \epsilon$ is the value of the d -level splitting under the influence of the crystalline electric field, roughly the order of the bandwidth. It is reasonable to assume that ξ for the $5d$ band does not differ too much from its atomic value. Moreover, for the compound (La_{1-x}Gd_x)Al₂ the $5d$ atoms La and Gd start with the same electronic configuration Xe $5d^1 6s^2$; for Gd we need only to add $4f$.⁷ Zipper assumes $\bar{\xi} \cong 0.256$ eV for Gd and $\Delta \epsilon \sim 3$ eV and estimates

$$g_d \cong 1.833.$$

Again, we treat the $5d$ -band electrons for g -value calculations similar to the ionic case (e.g., $3d$ ions⁴⁰). It is obvious that for $5d^n$ and $n < 5$ one gets $g < 2$.⁴¹

It is the beauty of the bottleneck effect in the ESR of dilute alloys that for strong bottlenecks the combined resonance of the two subsystems (Gd³⁺ and CE) does have the "fingerprint" of the CE as well. We have

$$g_{eff} \simeq g_i + (g_d - g_i) \frac{g_i^2 \chi_e}{g_d \chi_i} \left[1 + \frac{\lambda g_e \chi_i}{g_i} \right]. \quad (16)$$

If we use as the g value of the conduction band $g_d = 1.833$ and $g_i = 1.993$, the Pauli susceptibility $\chi_e = 2 \times 10^{-4}$ emu/mol, and for χ_i the experimental susceptibility (see Sec. V), we get

$$g_{eff} = 1.96.$$

This is very close to the experimental result. Similar estimates have been made for other systems.²⁷

It is the authors' opinion that this latter interpretation due to spin-orbit effect in the conduction band is more plausible than an interpretation via different exchange interactions. Note that this interpretation of $g_{eff} < g_i$ is only valid for the bottleneck case; in the isothermal limit one has

$$g_{\text{eff}} \approx g_i(1 + \lambda\chi_e)$$

independent of g_e .

V. RESULTS AND ANALYSIS FOR $T \lesssim T_{\text{min}}$

In this section we want to analyze the linewidth data for $T \lesssim T_{\text{min}}$. As one can see, T_{min} , introduced in the ESR spin-glass literature, is not a unique quantity for our system; it depends on applied magnetic field and/or on the microwave frequency (Figs. 4–7 and column 4 in Table I). To discriminate between different theoretical explanations for the minimum in the linewidth we have measured the magnetization of the 3-, 6-, 8-at. % samples and determined the differential susceptibility $\tilde{\chi}$ at the applied field for each ESR experiment (Fig. 8). In the following paragraphs we show how the observed width depends on $\tilde{\chi}^{-1}(H_{\text{expt}})$.

In Sec. III with the use of molecular-field equations, and thereby implicitly assuming a Curie-Weiss susceptibility, we arrived at Eqs. (11) for the effective relaxation rate of the bottleneck mode. In this section we wish to use a similar formula for the analysis of data near T_C where the susceptibility is not a Curie-Weiss form; we reexamine the validity of the formula for $T \gtrsim T_C$, but outside any true critical region.

It is clear that with an external field and approaching T_C , the molecular-field assumptions will break down for spin-spin interactions but they should remain valid for spin-CE interactions. We follow the ideas of Blandin⁴² and assume that the principal effect in a spin-glass above T_C is the formation of regions of correlated spins. This has the effect of renormalizing out the larger local-moment–local-moment interactions and might as a first approximation be incorporated in the theory through a temperature- and field-dependent coefficient $\alpha(T, H)$,

$$\chi_i = \chi_i^0(1 + \lambda\chi_e + \alpha(T, H)\chi_i)$$

and

$$\chi_e = \chi_i^0(1 + \lambda\chi_i).$$

Following the same line of reasoning as in Sec. III,

$$\delta \equiv \delta_{iL} \frac{\chi_i^0}{\chi_i} + \delta_{eL} \frac{\chi_e^0}{\chi_i} \quad (17a)$$

or

$$\Delta H \equiv \frac{\hbar\delta}{g\mu_B} = (a_0 + bT) \frac{\chi_i^0}{\chi_i}. \quad (17b)$$

Thus the linewidth depends on χ_i^{-1} , where χ_i is the susceptibility of the spin-glass. Since the external

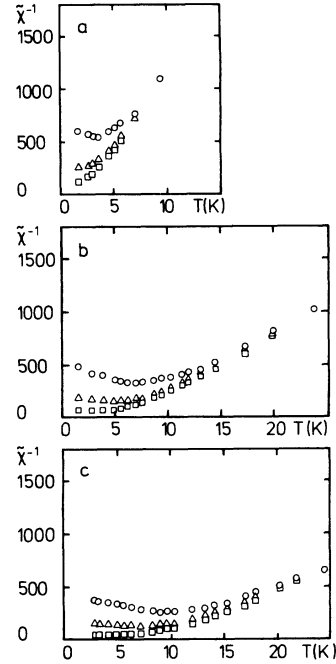


FIG. 8. Plot of the inverse differential susceptibilities $\tilde{\chi}$ of $(\text{Gd}_x\text{La}_{1-x})\text{Al}_2$ for (a) $x=3$ at. %, (b) $x=6$ at. %, and (c) $x=8$ at. %. Data were taken at 400 G (\square), 1200 G (\triangle), and 3400 G (\circ), corresponding to 1-, 3-, and 9-GHz resonance fields.

field H_0 is quite large it is important to decide whether χ_i is the true $\chi_i = (M/H)$ or the differential $\tilde{\chi} = \partial M / \partial H$ susceptibility. We argue that since what is important is the response of the system to an additional small field \vec{h}_{rf} in a system in which clusters begin to form and freeze, so it is the differential susceptibility which best represents the spins which are free to respond to the rf field.⁹ Accordingly we shall compare the inverse differential susceptibility $\tilde{\chi}^{-1}$ with the thermal broadening of our samples in the region $T \approx T_C$.

There is one further complication which we wish to add to the analysis. The lattice rate δ_{iL} which enters (17) is the motionally narrowed internal (anisotropy) field distribution. Any component of this or any other field distribution which fluctuates on a length greater than the characteristic spin-diffusion length l_s of the system will not suffer motional narrowing. One might view each piece of the sample with a size l_s as a separate system. It is clear that sufficiently long-range fluctuations in the field, such as, for example, those produced by demagnetization fields, will not be narrowed and will simply broaden the line by some amount a'_0 , and therefore⁴³

$$\Delta H = a'_0 + (a''_0 + bT)\chi_i^0\tilde{\chi}_i^{-1}. \quad (18)$$

As we have discussed in Sec. II and Appendix A

we know roughly the effect on line broadening due to demagnetization. This has been subtracted from the experimental data of the 6- and 8-at. % samples. The result is shown as the solid line in Fig. 9. Applying the ideas developed in Sec. III and the preceding paragraphs we used the experimental (differential) susceptibility $\tilde{\chi}_i$ in formula (18). The only fit parameters are a'_0 , a''_0 , and b . In Fig. 9 we used the thermal broadening at high T (not shown in the figures) from Table I. The main point which favors this analysis is the fair agreement for the field dependence of the minimum linewidth. For $T < T_{\min}$ no good agreement can be expected since the assumption of Sec. III, which has been used in this section too, may be valid only for $T \geq T_{\min}$. Note there is no free parameter to shift the minimum, and the experimental ESR results reflect the properties of χ^{-1} (Fig. 8). The fits for 3 and 15 at. % yield qualitatively similar results. However, the 3-at. % sample does not have such a strong bottleneck and the 15-at. % sample shows tentatively long-range ferromagnetic properties.

We now turn to the field shift. It is suggestive from the preceding paragraph that the internal magnetization of the Gd ions also play the dominant role in the line shift. The frequency-independent shift of the resonance (Figs. 4–7) supports this idea. We discuss in detail the 6-at. % sample (Fig. 5). There are differences in δH_{res} for the four frequencies; the highest frequency (\times) shows the largest shift. But this is a small effect (see next paragraph) and far from a proportionality with respect to the frequency. For 1 GHz (\square) one has, at $T = 2.5$ K, a shift of $\delta H_{\text{res}} \approx -130$ G; for 3 GHz, ≈ -150 G; for 9 GHz, ≈ -170 G; for 35 GHz, ≈ -210 G. One is forced to conclude that an internal magnetization with a field of $\delta \vec{H}_{\text{res}}$ parallel to \vec{H}_{ext} reduces the applied field by roughly 130 to 210 G to satisfy the resonance condition for $g = 2$. Again we feel that this is one main issue of the present investigation. It seems that similar experiments are necessary for other systems^{6,9,11,13} as well. There are no experimental points at lowest temperatures for the squares. This is due to the fact that for $H_{\text{res}} \equiv H_{\text{loc}} \approx 400$ G and a shift of $\delta H_{\text{res}} = -200$ G the applied field is very small, $H_{\text{ext}} \approx 200$ G, but the linewidth is large $\Delta H > 200$ G. This almost zero-field resonance can be analyzed, but many assumptions are necessary; this reduces the utility of such data.

The origin of the field shift can be investigated in a more quantitative fashion. The small differences in $\delta H_{\text{res}}(\nu)$ mentioned above suggest one of two interpretations: (1) a constant field shift superposed by a g shift, or (2) a full field shift due to an internal magnetization $M_i(H_{\text{ext}}, T)$. In Fig. 10 we compare

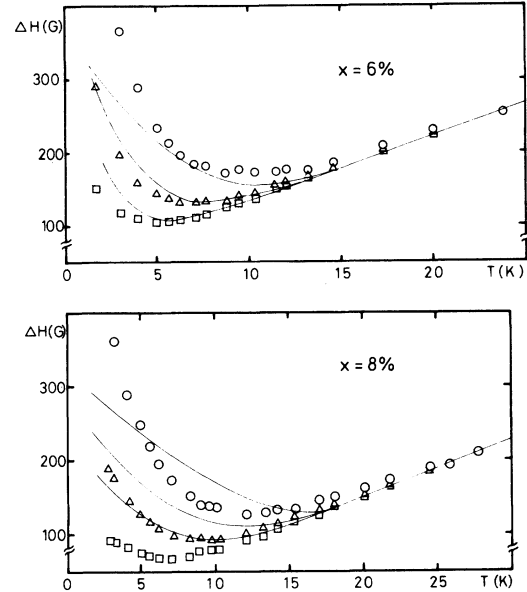


FIG. 9. Calculated linewidth according to Eq. (18) for $(La_{1-x}Gd_x)Al_2$ and $x = 0.06$ and 0.08 . Solid line shows the experimental behavior of ΔH (Figs. 5 and 6), but is corrected for the described demagnetization effect. Symbols (see Fig. 4) are now used for the calculated values of the linewidth (Sec. V). Fit parameters according to Eq. (18) and for 6 at. % (8 at. %) are $b = 8.9$ (7.7) G/K, $a'_0 = 70$ (40) G, and $a''_0 = 130$ (140) G. Note that χ_i^0 is Curie (not Curie-Weiss) susceptibility [Eq. (8)].

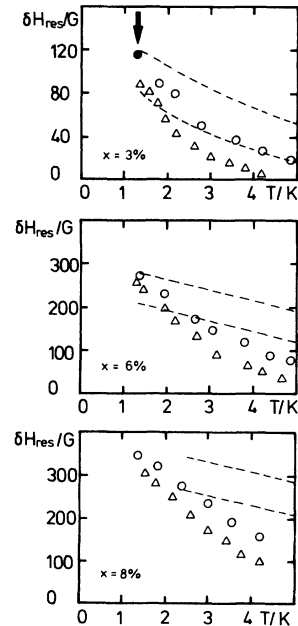


FIG. 10. Comparison of δH_{res} (points) with the behavior of the magnetization (dashed lines). For the values of the magnetization a fixed scaling factor is used which adjusts the values of M and δH_{res} for 3 at. %, 1.3 K, and 9 GHz only. For symbols see Fig. 4.

the experimental magnetization $M(H_{\text{ext}}, T)$ (dashed line) with δH_{res} for three concentrations. The only scaling for 3, 6, and 8 at. % and for both frequencies 3 and 9 GHz was to adjust the magnetization for 3 at. %, 1.3 K, and 9 GHz (solid circle, arrow). It is interesting how well the whole scheme fits: (a) The magnetization scales with δH_{res} (1.3 K) for 3, 6, and 8 at. %, (b) $M(3.4 \text{ kG})$ (upper line) and $M(1.2 \text{ kG})$ (lower line) at 1.3 K follow roughly (within a factor of 2) the resonance shift δH_{res} (9 GHz) and δH_{res} (3.2 GHz), however, (c) the temperature dependence clearly indicates the $\delta H_{\text{res}}(T)$ is not associated with the bulk magnetization $M(T)$. $\delta H_{\text{res}}(T)$ decreases much faster with increasing temperature, or (d) coming from high temperatures the bulk magnetization increases much slower than what is seen microscopically in the resonance. This—possibly critical—increase of δH_{res} cannot be interpreted in terms of a g shift. There is not a factor of 3 difference between \circ and \triangle .

VI. LOW-TEMPERATURE RESULTS $T < T_c$

The low-temperature ESR experiments are rather incomplete; we measured only the 6-at. % sample down to 100 mK. As is explained in the Introduction, the $T < T_c$ regime is not the focal point of the present investigation. The results will have only tentative character. In the next section we will discuss more details of a frequency-dependent cusp temperature $T_c(\nu)$.¹⁴ Here T_c will be taken as the value of $\sim 10 \text{ Hz}$, and for 6 at. % one gets $T_c \approx 1.6 \text{ K}$ (Ref. 15) in agreement with our own χ^{ac} experiments. Figure 11 shows the results. We were able to follow the resonance continuously from 100 mK up to 2–3 K under the same experimental conditions (^3He - ^4He dilution refrigerator²⁶). The line shape, line position, and linewidth do not depend on field cooling (FC) or zero-field cooling (ZFC).^{1,2,44} The width ΔH and shift δH_{res} become constant at $T < 300 \text{ mK}$. No time-dependent effect can be observed in our experiment. However, caution has to be taken since we are not able to measure short-time irreversibilities. For example a FC experiment is performed in the following way: At 4 to 5 K a field of 11 kG is applied, then the sample is cooled to 100 mK. Now the field is reduced to H_{res} very slowly because $\Delta H/\Delta t$ heats the sample. It typically takes 10 to 15 min.

VII. DISCUSSION

First we want to describe phenomenologically the difference in the experimental results of $(\text{LaGd})\text{Al}_2$ with respect to the prototype CuMn : Previously published ESR experiments in the high-temperature regime ($T > T_c$) of CuMn have been performed essentially at one frequency. In the present investi-

gation we showed that the minimum of the experimental linewidth and the upturn at lower T depends on many parameters (i.e., the actual susceptibility at H_{res} demagnetizing effect, etc.), which have to be eliminated first before discussing critical behavior. We also did show that no divergence appears for CuMn in the 9-GHz ESR.^{2,45} However, for low-field (-frequency) ESR (1, 3, and 4 GHz) in CuMn cooling down from high temperatures the signal disappears (enormous broadening and decreasing intensity) at $T \approx T_c/2$.⁴⁴ This is clearly different in $(\text{LaGd})\text{Al}_2$: We are able to follow the resonance continuously down to 100 mK. In addition the signal for $(\text{LaGd})\text{Al}_2$ does not depend on FC or ZFC of the sample. Both facts can easily be explained by the difference of the thermoremanent magnetization (TRM) and isothermremanent magnetization (IRM) for both systems: For CuMn at liquid-helium temperature the TRM is always larger than the IRM for fields of $H \leq 10 \text{ kG}$; for $(\text{LaGd})\text{Al}_2$, on the contrary, the TRM and IRM curves meet already at $H \approx 700 \text{ G}$ and $T = 80 \text{ mK}$. Since we worked $T \gg 80 \text{ mK}$ and $H \geq 700 \text{ G}$, we did not expect variations in the ESR signal for FC and ZFC conditions. For the same reason, we did not observe time-dependent effects.

In the previous sections it has been emphasized that the shift in the line position is principally due

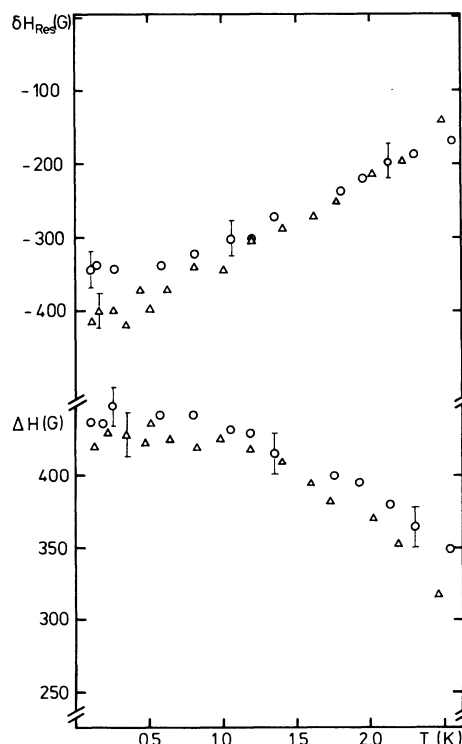


FIG. 11. Low-temperature data of linewidth and deviation of resonance field for $(\text{Gd}_{0.06}\text{La}_{0.94})\text{Al}_2$. See Fig. 5.

to an internal field rather than a change in the g factor. As in other studies we associated this with an anisotropy energy and the DM mechanism. We observe that the low-temperature $T < T_C$ shift and linewidth are correlated; the larger the shift the larger the linewidth. This suggests to us that the linewidth and shift both have as their origin the DM anisotropy energy. By inference the same is probably true for $T > T_C$ and in part justifies our assumption that this is the case in Sec. III. It is also implied that the onset of the shift and the broadening not associated with the (χ_i^0/χ_i) effect is caused by short-range correlations of the type already discussed. Field-shifted spin-wave modes will develop when correlation effects become sufficient; these modes coupled to the rest of the system will lead to a temperature-dependent shift and associated width above T_C but within the critical region. In the absence of any suitable theory we simply observe that our lowest-frequency data, and therefore that taken in the lowest external field, imply a critical region extending to some 3 times the freezing temperature.

At present, the connection between the microscopic picture of anisotropy^{4(c)} and the macroscopic parameters K_1 and K_2 for unidirectional and uniaxial effects is very vague. It is not the purpose of the present investigation to resolve this problem for (LaGd)Al₂. However, we did show that the spin-orbit interaction entered twice in our discussion:

(1) The spin-orbit scattering rate of essentially the $5d$ -band electrons for few percent Gd in LaAl₂ is in the order of 10^{12} sec⁻¹ (see Sec. III). The spin-flip lifetime δ_{eL} is of some interest because it is related to the virtual bound-state properties,⁴⁶

$$\delta_{eL} \langle \tau_{Tr} \rangle = (\pi/3) l(l+1) \lambda_{\text{eff}}^2 N_{\text{imp}}(E_F) / \Delta. \quad (19)$$

From band-structure calculations³⁹ it is concluded that the electrons at E_F have large La d components. The density of the subband is roughly $N_{\text{imp}}(E_F) \approx 0.3$ state/eV. The width of the valence-band state may be $\Delta \approx 2-3$ eV.³⁹ $\langle \tau_{Tr} \rangle$ can be determined from the Dingle temperature of de Haas-van Alphen experiments. For high-quality single crystals with a resistivity ratio of 10^3 one gets $T_D \approx 1$ K,⁴⁷ and for few at. % Gd in polycrystalline LaAl₂, $T_D \approx 10-30$ K are very likely. With those numbers one is able to calculate the effective spin-orbit-scattering parameter—the relevant quantity for the DM mechanism—to be (in eV)

$$\lambda_{\text{eff}} \approx 0.29.$$

(2) A cross check of these numbers is the effective g value at higher temperature in our system. This has been described in Sec. IV. The agreement for the parameters used above is surprisingly good.

The discussion so far is predicted upon the assumption of a phase transition at T_C . What inferences can be made if instead we follow Tholence¹⁴ and analyze our data in terms of a Fucher law? In this approach the observed temperature T_C depends upon the observation frequency. Explicitly,

$$T_C = T_0 - \frac{E_a/k}{\ln(\nu/\nu_0)}, \quad (20)$$

where according to Tholence, $\nu_0 = 10^{13}$ sec⁻¹, and for LaAl₂, $T_0 = 0$ when the above reduces to an Arrhenius law. For our 6-at. % sample, and with the use of the T_C at 16 Hz to determine (E_a/k) , we find the values of T_C listed in Table II for our various microwave frequencies. More than a 50% or almost 2.5-K increase in passing from the lowest to highest frequencies is predicted. And while the T_C at 16 Hz is 1.6 K the T_C at 1 GHz should be more than twice as large. Except with the extreme identification of T_C with the first significant shift δH_{res} neither the line-shift nor the linewidth data are compatible with such a strong frequency dependence of T_C .

ACKNOWLEDGMENT

This work was in part supported by Deutsche Forschungsgemeinschaft Sonderforschungsbereich 161 and NATO Grant No. 49.82. We would like to thank P. Beck, R. Parks, and A. Fert for helpful discussions and M. Hardiman and R. Orbach for communicating to us their AgMn results prior to publication. One of us (S.E.B.) thanks the Sonderforschungsbereich 161 for financial support during his stay at the Freie Universität Berlin.

APPENDIX A: DEMAGNETIZATION EFFECTS IN ESR EXPERIMENTS

Since in some of the recent papers this effect has not been discussed, we reevaluate it again⁴⁸ and give numbers for our system. The local field H_{loc} acting on an individual ion is given by the superposition of

TABLE II. This table shows the calculated values of T_C of (La_{1-x}Gd_x)Al₂ for various concentrations x and frequencies according to Eq. (20). Low-frequency corresponds to an ac-susceptibility experiment, and the three high-frequency ones correspond to the L -, X -, and Q -band microwave frequencies.

ν (sec ⁻¹)	T_C (K)		
	$x = 3$ at. %	$x = 6$ at. %	$x = 8$ at. %
16	0.8	1.6	2.1
1×10^9	2.0	4.6	6.1
1×10^{10}	3.1	5.5	8.1
3.5×10^{10}	3.4	6.7	9.9

the applied field H_{ext} and the field produced by the magnetic moments⁴⁹

$$H_{\text{loc}} = H_{\text{ext}} - 4\pi NM + \frac{4}{3}\pi M + \sum_K H_K, \quad (\text{A1})$$

where M is the magnetization of the sample, N is the demagnetization factor, and H_K is the field produced by a moment on the lattice site K . Because of the cubic symmetry and the statistical spread impurities the last sum in Eq. (A1) vanishes and one gets

$$H_{\text{loc}} = H_{\text{ext}} - (N - \frac{1}{3})4\pi M. \quad (\text{A2})$$

In all ESR experiments one is looking for the "real" field for resonance H_{loc} rather than H_{ext} as the relevant field. For spheres ($N = \frac{1}{3}$) one has $H_{\text{loc}} = H_{\text{ext}}$; this on the average also holds for powder samples (within the restriction that the grains are "far away" from each other). Therefore, we corrected only the field for resonance of our cylinder sample used for the low-temperature experiments according to the formula for N of finite cylinders,⁵⁰

$$N \cong \frac{1}{2} \left[1 - \left(\frac{R}{d} \right)^2 \ln \frac{d}{r} \right], \quad (\text{A3})$$

where $2d$ is the length, R is the radius of the cylinder, and the applied field is perpendicular to the cylinder axis. Indeed experimentally we found different resonance fields for the cylinder which coincided with the one for powder after correction.

The effect of demagnetization on the linewidth and line shape is discussed in detail elsewhere.²⁷ Here we give only a rough estimation for the linewidth effect assuming that our powder consists of randomly orientated ellipsoids. The actual local field in a particular ellipsoid depends on the geometry and orientation of this grain. If the length of the half-axes of an "average grain" are a and b , one has a distribution of local fields and therefore an additional contribution $\Delta H'$ to the linewidth corresponding to different orientations which is of the order

$$\Delta H' = H_{\text{loc}||a} - H_{\text{loc}||b} = (N_a - N_b)4\pi M. \quad (\text{A4})$$

Here N_a and N_b are the demagnetization factors corresponding to the a and b axes.

For our powder we assume an a/b ratio of the order of 2 corresponding to $\Delta N \cong 0.25$.⁵¹ From this one gets an extra contribution to the linewidth:

$$\Delta H' \cong \pi M. \quad (\text{A5})$$

In Fig. 12 we show as an example the magnetization curve of the 6-at. % sample at low temperatures where the demagnetization effects are important. From this one determines, that for the 1.5-K and 3.4-kG applied field (X band), the correction for the

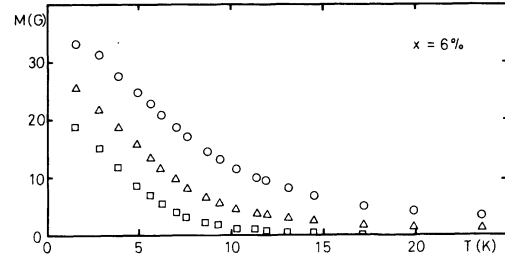


FIG. 12. Following Eqs. (A2) and (A4) we show $M(T)$ for the 6-at. % sample. Additional line broadening due to demagnetization effects equals $\Delta H' \approx 4\pi M \Delta N \approx \pi M$. Experimental linewidth (solid line) in Fig. 9 is corrected for this. For symbols see Fig. 4.

field for resonance (cylinder versus powder) is ~ 53 G ($R = 1.9$ mm, $d = 8.5$ mm) and the additional linewidth $\Delta H'$ is on the order of 100 G.

APPENDIX B: LINE BROADENING DUE TO INHOMOGENEOUS FIELD DISTRIBUTION

The purpose here is to demonstrate that the broadening due to an internal field distribution when motionally narrowed by cross relaxation can be correctly accounted for by a term (δ_{iL}) in the Bloch-Hasegawa equations. For the present purpose ignore the existence of correlated spins and assume, as an example, a field distribution with only two values $\pm h_0$. The equations are identical to those for hyperfine splitting. The linearized Bloch-Hasegawa equations are

$$\begin{aligned} \frac{d}{dt} M_1^+ &= \left[i[\omega_i(1 + \lambda\chi_e) + \omega_0] - \delta_{ie} - \frac{1}{2\tau_i} \right] \delta M_1^+ \\ &+ \frac{1}{2\tau_i} \delta M_2 + \frac{g_i}{2g_e} \delta_{ei} \delta M_e^+ \end{aligned} \quad (\text{B1a})$$

and

$$\begin{aligned} \frac{d}{dt} M_2^+ &= \left[i[\omega_i(1 + \lambda\chi_e) - \omega_0] - \delta_{ie} - \frac{1}{2\tau_i} \right] \delta M_2^+ \\ &+ \frac{1}{2\tau_i} \delta M_1 + \frac{g_e}{2g_i} \delta_{ei} \delta M_e^+, \end{aligned} \quad (\text{B1b})$$

where $\omega_0 = g_i \mu_B h_0$, where the total local-moment magnetization $M_i^+ = M_1^+ + M_2^+$, and where

$$\delta M_{1(2)} = [M_{1(2)}^+ - \frac{1}{2}\chi_i^0(h_{\text{rf}} + \lambda M_e^+ + \alpha M_i)] . \quad (\text{B1c})$$

Adding and subtracting give

$$\begin{aligned} \frac{d}{dt} M_i^+ &= [i\omega_i(1 + \lambda\chi_e) - \delta_{ie}] \delta M_i^+ \\ &+ \frac{g_i}{g_e} \delta_{ei} \delta M_e^+ + i\omega_0 A_i^+ \end{aligned} \quad (\text{B2a})$$

and

$$\frac{d}{dt}A_i^+ = \left[i\omega_i(1 + \lambda\chi_e) - \delta_{ie} - \frac{1}{\tau_i} \right] A_i^+ + i\omega_0\delta M_i^+ . \quad (\text{B2b})$$

Assuming the relaxation between M_1 and $M_2(1/\tau_i) \gg \omega_0$ (and δ_{ie}), we can eliminate A_i^+ ,

$$A_i^+ \simeq i\omega_0\tau_i\delta M_i^+ . \quad (\text{B3})$$

Hence

$$\begin{aligned} \frac{d}{dt}M_i^+ &= [i\omega_i(1 + \lambda\chi_e) - \delta_{ie} - \delta_{il}]\delta M_i^+ \\ &+ \frac{g_i}{g_e}\delta_{ei}\delta M_e^+ , \end{aligned} \quad (\text{B4})$$

where

$$\delta_{il} = \omega_0^2\tau_i = \frac{1}{2} \langle (\Delta\omega_i)^2 \rangle \tau . \quad (\text{B5})$$

The important point relative to the factor of (χ_i^0/χ_i) is the appearance of δM_i^+ , rather than simply M_1^+ in Eqs. (B2b) and hence (B4). This stems from the fact that the linearized torque term, e.g.,

$$\vec{M}_1 \times (\vec{H}_{\text{ext}} + h_0\hat{z} + \lambda\vec{M}_e + \alpha\vec{M}_i) ,$$

becomes $i[\omega_i(1 + \lambda\chi_e) + \omega_0]\delta M_i^+$ and is also proportional to the deviation from equilibrium and not simply M_1^+ . It is not difficult to generalize the above to a continuous distribution simply by replacing ω_0^2 in (B5) by the second moment as is implied by the extreme right-hand side of this equation.

- ¹P. Monod and Y. Berthier, *J. Magn. Magn. Mater.* **15-18**, 149 (1980).
²S. Schultz, E. M. Gullikson, D. R. Fredkin, and M. Tover, *Phys. Rev. Lett.* **45**, 1508 (1980); *J. Appl. Phys.* **52**, 1776 (1981).
³J. Owens, M. E. Browne, V. Arp, and A. F. Kip, *J. Phys. Chem. Solids* **2**, 85 (1957).
⁴(a) A. Fert and P. M. Levy, *Phys. Rev. Lett.* **44**, 1538 (1980); (b) P. M. Levy and A. Fert, *J. Appl. Phys.* **52**, 1718 (1981); (c) P. M. Levy, C. Morgan-Pond, and A. Fert, *J. Appl. Phys.* **53**, 2168 (1982).
⁵M. B. Salamon and R. M. Herman, *Phys. Rev. Lett.* **41**, 1506 (1978).
⁶M. B. Salamon, *Solid State Commun.* **31**, 781 (1979); *J. Magn. Magn. Mater.* **15-18**, 147 (1980).
⁷E. D. Dahlberg, M. Hardiman, R. Orbach, and J. Souletie, *Phys. Rev. Lett.* **42**, 401 (1979).
⁸E. D. Dahlberg, M. Hardiman, and J. Souletie, *J. Phys. (Paris) Lett.* **39**, L-389 (1978).
⁹D. Varknin, D. Davidov, G. J. Nieuwenhuys, F. R. Hoekstra, G. E. Barberis, and J. A. Mydosh, *Physica* **108B**, 765 (1981).
¹⁰B. R. Coles, B. V. B. Sarkissian, and R. H. Taylor, *Philos. Mag. B* **37**, 489 (1978).
¹¹A. P. Malozemoff and J. P. Janet, *Phys. Rev. Lett.* **39**, 1293 (1977), J. P. Janet and A. P. Malozemoff, *Phys. Rev. B* **18**, 75 (1978).
¹²M. Zomack and K. Baberschke, *Physica* **108B**, 773 (1981).
¹³A. P. Malozemoff, L. Krusin-Elbaum, and R. C. Taylor, *J. Appl. Phys.* **52**, 1773 (1981).
¹⁴H. v. Löhneysen, J. L. Tholence, and R. Tournier, *J. Phys. (Paris)* **C6**, 922 (1978); J. L. Tholence, *Solid State Commun.* **35**, 113 (1980).
¹⁵H. v. Löhneysen, J. L. Tholence, and F. Steglich, *Z. Phys.* **29**, 319 (1978); C. D. Bredl, F. Steglich, H. v. Löhneysen, K. Matko, *J. Phys. (Paris)* **C6**, 925 (1978).
¹⁶H. v. Löhneysen and J. L. Tholence, *J. Magn. Magn. Mater.* **15-18**, 171 (1980).

- ¹⁷(a) G. Koopman, U. Engel, K. Baberschke, and S. Hufner, *Solid State Commun.* **11**, 1197 (1972); (b) D. Davidov, A. Chelkowski, C. Rettori, R. Orbach, and M. B. Maple, *Phys. Rev. B* **7**, 1029 (1973).
¹⁸K. Baberschke, *Z. Phys. B* **24**, 53 (1976).
¹⁹K. Baberschke, B. Bacher, and S. E. Barnes, *Phys. Rev. B* **21**, 2666 (1980).
²⁰A. W. Stewart, *Aust. J. Phys.* **33**, 1049 (1980).
²¹E. Zipper, *J. Phys. F* (in press). We would like to thank E. Zipper for sending us the manuscript prior to publication.
²²It is interesting to note that in E. Dorman and V. Jaccarino, *Phys. Lett.* **48A**, 81 (1974); E. Dorman, D. Hone, and V. Jaccarino, *Phys. Rev. B* **14**, 2714 (1976), wherein the authors found a large increase of the linewidth by decreasing the temperature for $3 \leq T/T_C < 10$ and that this "bears no relation to critical phenomena."
²³Y. v. Spalden and K. Baberschke, *Physica* **107B**, 599 (1981); J. Nagel, K. Baberschke, and E. Tsang, *J. Magn. Magn. Mater.* **15-18**, 1512 (1980).
²⁴J. B. Boyce and K. Baberschke, *Solid State Commun.* **39**, 181 (1981).
²⁵E. Dartye, H. Bouchiat, and P. Monod (unpublished).
²⁶H. Peter, D. Shaltiel, J. V. Wernick, H. J. Williams, J. B. Bock, and R. C. Sherwood, *Phys. Rev.* **126**, 1395 (1962).
²⁷George Mozurkewich, H. J. Ringermacher, and D. J. Bolef, *Phys. Rev. B* **20**, 1, 33 (1979).
²⁸A. J. Larkin and D. E. Khmel'nitskii, *Zh. Eksp. Teor. Fiz.* **58**, 1789 (1970) [*Sov. Phys.—JETP* **31**, 958 (1970)].
²⁹K. Matho, in *Proceedings of the 15th International Conference on Statistical Physics*, Haifa, 1977 (unpublished).
³⁰F. J. Dyson, *Phys. Rev.* **89**, 689 (1951). For details see, e.g., K. Baberschke and E. Tsang, *Phys. Rev. Lett.* **45**,

- 18 (1980); 45, 512 (1980).
- ³¹Y. v. Spalden and K. Baberschke, *J. Magn. Magn. Mater.* 23, 183 (1981).
- ³²For details and notation, see Refs. 18 or 49.
- ³³There exists no common use of notation and symbols. We will use as a relaxation rate $\delta_{ab}(a \rightarrow b)$ instead of $1/T_{ab}$. The subscripts are read as i for impurity (i.e., Gd spin), e for CE, L for lattice = bath, \vec{S} for the local spin operator, and $\vec{\sigma}$ for the CE spin operator. The exchange interaction we define as $H_{ex} = -J_{st}\vec{S}\vec{\sigma}$ (no factor of 2). Consequently, the Korringa rate is given by $\hbar\delta_{ie} = \pi(\rho J)^2 kT = g_{eff}\mu_B \Delta\tilde{H}$, $\Delta\tilde{H}$ being the relaxation part of the linewidth.
- ³⁴R. H. Taylor, *J. Phys. F* 3, L110 (1973).
- ³⁵S. E. Barnes, *Adv. Phys.* 30, 801 (1981).
- ³⁶B. Maple, thesis, University of California at San Diego La Jolla, 1969 (unpublished).
- ³⁷For a review, see R. H. Taylor, *Adv. Phys.* 24, 681 (1975).
- ³⁸A. Troper, D. L. T. de Menezes, and A. A. Gomes, *J. Phys. F* 4, 2457 (1979).
- ³⁹A. Hasegawa and A. Yanase, *J. Phys. F* 10, 847 (1980).
- ⁴⁰A. Abragam and B. Bleaney, *ESR in Transition Metals* (Clarendon, Oxford, 1970).
- ⁴¹For $n > 5$, $PdMn$ is an excellent example. Alquie [Ph.D. thesis, Université de Paris, 1977 (unpublished)] has determined the conduction electron g value to be $g_e = 2.245$.
- ⁴²A. Blandin, *J. Appl. Phys.* 89, 1285 (1968).
- ⁴³Note that in formulas (12) and (17b), always $a_0 = (\hbar/g\mu_B)\delta_{iL}$ holds. But (12) is valid only for $T \gg \Theta$.
- ⁴⁴F. R. Hoekstra, K. Baberschke, M. Zomack, and J. Mydosh, *Solid State Commun.* 43, 109 (1982).
- ⁴⁵F. Hoekstra, private communication.
- ⁴⁶R. Orbach, in *Proceedings of the 14th International Conference on Low-Temperature Physics, Otaniemi, 1975*, edited by M. Krusius and M. Vuorio (North-Holland, Amsterdam, 1975), p. 375.
- ⁴⁷J. Reichelt, thesis, University of Göttingen, 1981 (unpublished).
- ⁴⁸See Ref. 27 and Refs. 1–3 therein.
- ⁴⁹C. Kittel, *Introduction to Solid Physics* (Wiley, New York, 1976), Chap. 13. The electrical case discussed there can be easily translated into the magnetic one.
- ⁵⁰L. D. Landau and E. M. Lifschitz, *Electrodynamics of Continuous Media* (Pergamon, New York, 1960).
- ⁵¹Values for N are calculated in J. A. Osborn, *Phys. Rev.* 67, 351 (1945).